Fourier Transform Emission Spectroscopy of a New $^2\Phi$–$1\,^2\Delta$ System of VO

R. S. Ram,* P. F. Bernath,*,† S. P. Davis,‡ and A. J. Merer§

*Department of Chemistry, University of Arizona, Tucson, Arizona 85721; †Department of Chemistry, University of Waterloo, Waterloo, Ontario, Canada N2L 3G1; ‡Department of Physics, University of California, Berkeley, California 94720; and §Department of Chemistry, University of British Columbia, 2036 Main Mall, Vancouver, British Columbia, Canada V6T 1Z1

High-resolution emission spectra of VO have been recorded in the region 3400–19 400 cm^{-1} using a Fourier transform spectrometer. The molecules were observed from the reaction of VOCl$_3$ with active nitrogen. Two new bands, with origins near 5539.46 and 5551.69 cm^{-1}, are assigned as the 0–0 bands of the $^2\Phi_{5/2}$–$^2\Delta_{3/2}$ and $^2\Phi_{7/2}$–$^2\Delta_{5/2}$ spin–orbit components (respectively) of a $^2\Phi$–$1\,^2\Delta$ electronic transition of VO. A rotational analysis of both subbands has been carried out and spectroscopic constants have been extracted. The $1\,^2\Delta$ state is known from the previous analysis of the near infrared doublet transitions of VO and the new $^2\Phi$ excited state has rotational constants very similar to those of another $^2\Phi$ state observed previously [Merer *et al.*, *J. Mol. Spectrosc.* **125,** 465 (1987)]. © 2002 Elsevier Science (USA)

INTRODUCTION

Over the past two decades considerable progress has been made in the characterization of diatomic species containing transition metal elements, partly motivated by their chemical (*1, 2*) and astrophysical (*3, 4*) importance. For example, transition metal monoxides can be used as model systems for transition metal bonding on surfaces. Because of the high cosmic abundances of 3*d* transition metal elements, several transition metal monoxides have been found in the atmospheres of cool stars. For example, TiO (*5, 6*) and VO (*7–10*) have been found in the atmospheres of cool M-type stars and ZrO (*10*) has been identified in S-type stars. In fact, VO provides the basis for the spectral classification of late M-type stars (*11*).

Vanadium oxide solids are also of industrial importance. VO and other oxides of vanadium such as VO$_2$ and V$_2$O$_2$ are of considerable interest due to their use in optical devices, semiconductors, catalysts, and coatings (*12–17*). Because of its high corrosion resistance at normal temperatures, vanadium is used to produce rust-resistant industrial devices. At high temperatures vanadium starts oxidizing and therefore the study of reaction dynamics and oxidation processes of gas phase clusters of vanadium is also of industrial interest (*18*).

VO is the most extensively studied molecule in the Group 5 oxide family (VO, NbO, and TaO) and its ground state is well established as $X\,^4\Sigma^-$ from numerous theoretical (*19, 20*) and experimental (*21–26*) studies. The visible and near infrared spectra of VO consist of three strong transitions which have been identified as $A\,^4\Pi$–$X\,^4\Sigma^-$ (*21*), $B\,^4\Pi$–$X\,^4\Sigma^-$ (*22–24*), and $C\,^4\Sigma^-$–$X\,^4\Sigma^-$ (*25, 26*). Vanadium has a high nuclear spin and a large nuclear moment, so the hyperfine structure is resolved in these transitions at high resolution, and hyperfine constants have been

determined in addition to the usual rotational constants. The near infrared region is rich with VO transitions which have been classified into two quartet–quartet and several doublet–doublet transitions (*27*). The near infrared quartet transitions originate from the $D\,^4\Delta$ state and terminate on the $A\,^4\Pi$ state and another low-lying $A'\,^4\Phi$ state and, therefore, the location of all low-lying quartet states is known relative to the ground state. A low-lying $^2\Sigma^+$ state has been identified from the analysis of the perturbations in the $B\,^4\Pi$–$X\,^4\Sigma^-$ transition (*23, 24*). Among the doublet transitions of VO, there are two $^2\Pi$–$^2\Delta$ transitions near 7200 cm^{-1} and 8126 cm^{-1} for which the common lower state is $1\,^2\Delta$. There is another doublet transition, which has been assigned as $2\,^2\Delta$–$1\,^2\Phi$, that does not have any state in common with the other two doublet transitions. Since the two groups of doublet–doublet transitions are not connected to the quartet manifold, the positions of the low-lying $1\,^2\Delta$ and $1\,^2\Phi$ states are not known with respect to the ground state.

Microwave spectra and the dipole moment have been measured for the $X\,^4\Sigma^-_{1/2}$ state using a pulsed-nozzle Fourier transform microwave spectrometer with a laser vaporization source (*28*). The Stark shifts of the hyperfine components of the $J = 3/2$–$1/2$ line have given the dipole moment of VO as 3.355 D (*28*). Lifetime measurements for the $A\,^4\Pi$, $B\,^4\Pi$, and $C\,^4\Sigma^-$ states have been performed using two-photon ionization in a molecular beam and lifetimes of $6 \pm 1\ \mu$s, $0.37 \pm 0.05\ \mu$s, and 73 ± 2 ns, respectively, have been obtained for these states (*29*). Several high-temperature vaporization, thermodynamic, and photoionization studies of VO have also been carried out in recent years (*30–32*). The thermodynamic properties of VO have been characterized by means of high-temperature mass spectrometry by Balducci *et al.* (*31*) and the dissociation energy, D_0(VO) = 625.5 $\pm$ 8.5 kJ/mol, obtained.

The ionization potential of VO has been measured to be 58 383(5) cm^{-1} by zero kinetic energy threshold photoelectron spectroscopy (*33*). The infrared (*17*) and ESR (*34*) spectra of VO and other oxides of vanadium such as VO$_2$ have been observed from the reaction of laser-ablated vanadium atoms with O$_2$ in solid argon and the ground state vibrational intervals for these species have been measured (*17*). VO molecules created by ablation have also been studied in presence of trapping magnetic fields after cooling them using a buffer gas (*35*). This method has been used to measure the rotational temperature and has also provided magnetic parameters for several optical transitions (*35*).

Theoretical studies of VO along with VS, ScO, and ScS, have been performed by Bauschlicher *et al.* (*20*) using the coupled pair functional method to predict the spectroscopic properties of a number of low-lying electronic states. A recent study of the photoelectron spectra of VO$^-$, VO$_2^-$, VO$_3^-$, and VO$_4^-$ (*36*) has given information about the low-lying states of the corresponding neutral molecules. For VO, a new electronic state which gives a strong peak at 5630 cm^{-1} has been assigned as a transition to the $^2\Sigma^-(\sigma\delta^2)$ state. A weaker peak at 14 920 cm^{-1} whose intensity varies with ionization wavelength in the expected way for loss of a δ electron from the ground state of VO$^-$ is tentatively assigned as a $^2\Phi$ state.

In the current work we have observed a new $^2\Phi$–$^2\Delta$ electronic transition of VO near 5550 cm^{-1} with the previously known $1^2\Delta$ state as its lower state. In this paper we report the rotational analysis of the 0–0 band of this system and provide improved spectroscopic constants for the $1^2\Delta$ state.

EXPERIMENTAL DETAILS

The VO molecules were formed in the reaction of a flowing mixture of VOCl$_3$ vapor and active nitrogen. The reaction vessel was a Pyrex tube 15 mm in diameter and 50 cm long, aligned along the optical axis of the spectrometer with one end placed against the entrance aperture. A roughing pump pumped full bore on the outlet nearest the spectrometer. At the far end, nitrogen was introduced after passing through a short section of quartz tubing where it was excited with a microwave discharge. The VOCl$_3$ vapor was introduced from a bottle of liquid (at room temperature) through another side tube whose inlet was located at the center of the main tube near the incoming active nitrogen. Beneath the entire reaction tube we placed a styrofoam boat filled with liquid nitrogen. The evaporating vapor flowed around the tube. The amount of cooling had a major effect on the intensity of the spectrum. Either too much or too little cooling reduced the intensity by almost an order of magnitude.

The spectra were recorded with the 1-m Fourier transform spectrometer associated with the McMath–Pierce telescope of the National Solar Observatory at Kitt Peak. The spectra in the interval 3400–19 400 cm^{-1} were recorded in two parts. For the region 3400–14 700 cm^{-1} the spectrometer was equipped with a CaF$_2$ beam splitter, RG715 red pass filters, and liquid-

nitrogen-cooled InSb detectors. The spectra were recorded by coadding four scans in about 1 h of integration at a resolution of 0.0156 cm^{-1}. For the 8700–19 400 cm^{-1} region, the spectrometer was equipped with a CaF$_2$ beam splitter, OG530 filters, and midrange silicon diode detectors. This time four scans were coadded in about 45 min of integration at a resolution of 0.025 cm^{-1}.

The spectral line positions were determined using a data reduction program called PC-DECOMP developed by J. Brault. The peak positions were determined by fitting a Voigt lineshape function to each feature. In addition to VO bands, VN and VCl bands were also present, along with V atomic lines. The CO 2–0 overtone band was present as an impurity. The VO spectrum was calibrated using the measurements of the 2–0 overtone lines of CO provided by Maki and Wells (*37*). The absolute accuracy of the wavenumber scale is expected to be on the order of $\pm$0.002 cm^{-1}. The rotational lines of the $^2\Phi$–$1^2\Delta$ transition of VO appear with a typical signal-to-noise ratio of 8 : 1 and have an approximate linewidth of 0.032 cm^{-1}. The precision of measurements of strong and unblended lines of VO is expected to be better than $\pm$0.003 cm^{-1}.

RESULTS AND DISCUSSION

Our spectra consist of several new bands of VO and VN and a recently reported $[7.0]^5\Delta$–$X^5\Delta$ transition of VCl (*38*) in the near infrared. Two new transitions of VN have been identified, the results will be published elsewhere (*39*). The new emission system of VO reported in the present paper is located in the region, 5400–5600 cm^{-1} and consists of two subbands with origins at 5539.46 and 5551.69 cm^{-1}. These subbands both have P, Q, and R branches, with no doubling even at the highest J values, and the relative intensities of the branches suggest that they should be assigned as the two spin–orbit components of a $^2\Phi$–$^2\Delta$ transition. After comparison of the combination differences of the states of this transition with the combination differences of other known doublet states (*27*), this transition has been assigned as a $^2\Phi$–$1^2\Delta$ with the lower $1^2\Delta$ state being common to the lower states of the two $^2\Pi$–$^2\Delta$ transitions near 7200 and 8100 cm^{-1}. The excited $^2\Phi$ state has rotational constants similar in magnitude to the $1^2\Phi$ state, observed previously by Merer *et al.* (*27*).

A part of the spectrum near the bandheads has been provided in Fig. 1 in which lines belonging to the head-forming R and Q branches have been marked. Lines up to $R(44.5)$, $P(43.5)$, and $Q(47.5)$ have been observed in the $^2\Phi_{5/2}$–$1^2\Delta_{3/2}$ subband while lines up to $R(38.5)$, $P(39.5)$, and $Q(41.5)$ have been observed in the $^2\Phi_{7/2}$–$1^2\Delta_{5/2}$ subband. Some broadening, presumably due to hyperfine effects, has been observed in the low J lines of the $^2\Phi_{5/2}$–$1^2\Delta_{3/2}$ subband. No vibrational bands other than 0–0 have been identified, which unfortunately means that the vibrational frequencies of the electronic states cannot be obtained. Also no cross transitions with $\Delta\Sigma \neq 0$ were observed in our spectra so that the spin–orbit intervals could not be determined
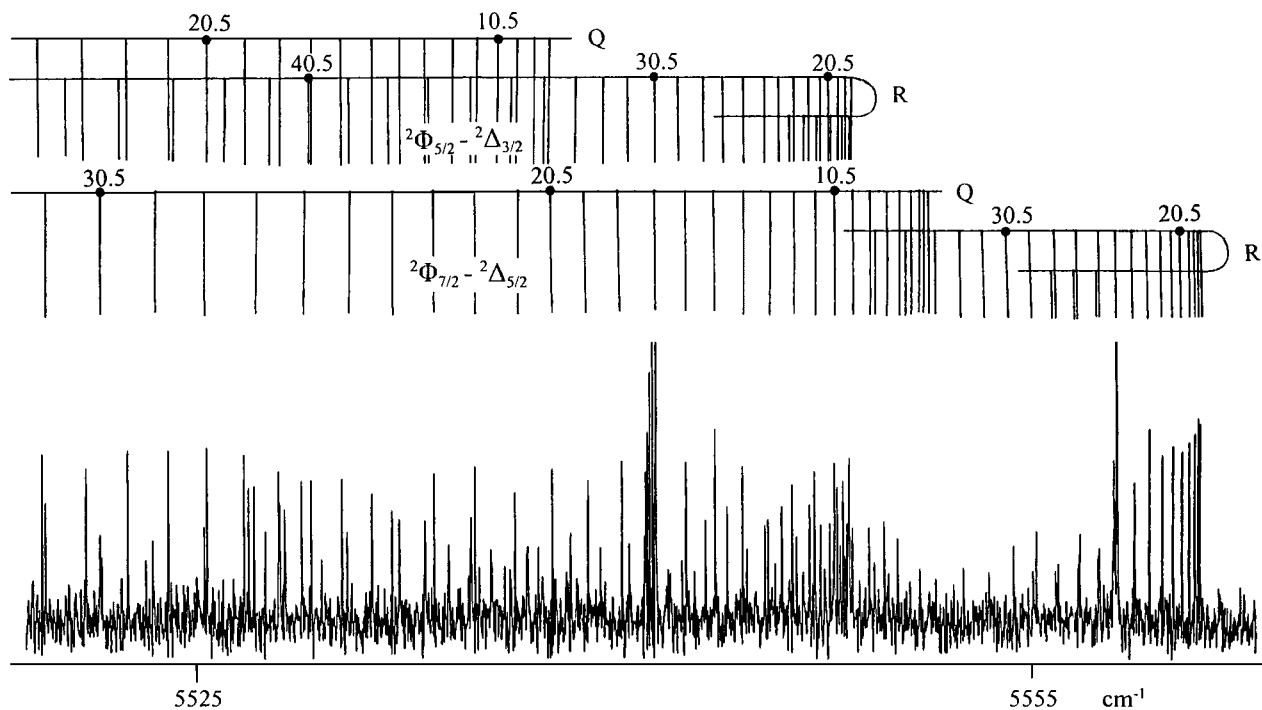
FIG. 1. An expanded portion of the new 0–0 band of VO near the R heads.

directly. The rotational constants for the two spin components of the observed states were determined by fitting the lines of both subbands separately using a simple term energy expression, although the observed electronic states most likely obey Hund's case (a) coupling:

$$F_v(J) = T_v + B_v J(J+1) - D_v[J(J+1)]^2 + H_v[J(J+1)]^3. \quad [1]$$

The rotational lines were given weights based on their relative intensity and extent of blending. The inclusion of the higher order constant H_v for both spin components of the lower $1\,^2\Delta$ state is a reflection of interactions of this state with other close-lying electronic states. In the final fit the combination differences for the $1\,^2\Delta_{3/2}$ and $1\,^2\Delta_{5/2}$ spin components for $v = 0$ from Merer *et al.* (*27*) were also included with appropriate weights. It seems that the high-J lines of the $1\,^2\Delta_{5/2}$ spin component are severely affected by interactions with other states since their inclusion in the fit dramatically increases the standard deviation. The lines with $J \geq 37.5$ were, therefore, heavily deweighted in the final fit. The observed line positions for the two subbands are provided in Table 1 and the molecular constants for the two spin components of the $^2\Phi$ and $1\,^2\Delta$ states are provided in Table 2.

At the initial stage of the analysis it was noted that the new $^2\Phi_{7/2}$ spin component has very similar rotational constants to the $1\,^2\Phi_{7/2}$ spin component initially observed by Merer *et al.* (*27*) in the analysis of the $2\,^2\Delta_{5/2}$–$1\,^2\Phi_{7/2}$ subband near 9600 cm^{-1}, although the constants for the new $^2\Phi_{5/2}$ spin component were

quite different from those of the $1\,^2\Phi_{5/2}$ spin component. We were therefore misled and believed that the excited state of the new transition was the $1\,^2\Phi$ state and the difference in the rotational constants of the two $^2\Phi_{5/2}$ spin components was due to an error in the vibrational numbering in the $2\,^2\Delta_{3/2}$–$1\,^2\Phi_{5/2}$ subband of Merer *et al.* (*27*). However, a more careful inspection of the combination differences for the $^2\Phi_{7/2}$–$1\,^2\Delta_{5/2}$ subband of the new transition revealed that there is a small but systematic difference between the combination differences of the two $^2\Phi_{7/2}$ spin components although the differences at lower J values were within the error limit. For example, the $\Delta_2 F(J)$ combination difference at $J = 17.5$ of the new $^2\Phi_{7/2}$ spin components differs by 0.011 cm^{-1} while that at $J = 31.5$ the discrepancy is 0.037 cm^{-1}, which is clearly outside the measurement error. On the other hand there is a very good agreement between the lower $1\,^2\Delta$ state combination differences obtained from the present data and those provided by the other near infrared transitions (*27*). This led us to conclude that the new $^2\Phi$ state is not the same as the $1\,^2\Phi$ state previously observed by Merer *et al.* (*27*), as was assumed erroneously at the start of the analysis.

At present we are not sure which of the two $^2\Phi$ states has been observed in the recent photoelectron spectrum of VO$^-$ (*36*) (and the $^2\Phi$ assignment itself is not completely secure). If the new $^2\Phi$ excited state is the one observed at 14 920 cm^{-1} in the anion photoelectron spectrum of VO$^-$ recorded by Wu and Wang (*36*) then we can determine the absolute energies of most of the doublet states (*27*) relative to the ground state (except for the $2\,^2\Delta$ and $1\,^2\Phi$ states). The observation of the new $^2\Phi$ state of VO

TABLE 1

Observed Line Positions (in cm^{-1}) for the $^2\Phi$–$1^2\Delta$ 0–0 Band of VO

J	R(J)	O-C	Q(J)	O-C	P(J)	O-C	R(J)	O-C	Q(J)	O-C	P(J)	O-C
			$^2\Phi_{5/2}$–$1^2\Delta_{3/2}$						$^2\Phi_{7/2}$–$1^2\Delta_{5/2}$			
2.5							5555.060	2				
3.5							5555.873	−5				
4.5							5556.633	−2	5550.928	20		
5.5							5557.331	3	5550.565	4		
6.5			5537.910	2			5557.952	−7	5550.158	8		
7.5	5546.260	9	5537.432	2			5558.536	11	5549.683	8		
8.5	5546.751	5	5536.883	−5			5559.033	4	5549.143	4		
9.5	5547.187	10	5536.279	−2			5559.471	2	5548.538	−1	5538.666	18
10.5	5547.537	−7	5535.609	−3	5524.723	7	5559.844	−2	5547.876	0	5536.956	11
11.5	5547.855	8	5534.883	5	5522.949	4	5560.157	−4	5547.153	4	5535.179	1
12.5	5548.088	1	5534.083	3	5521.119	8	5560.406	−5	5546.362	2	5533.346	−3
13.5	5548.260	−3	5533.216	−4	5519.225	11	5560.593	−6	5545.508	1	5531.450	−6
14.5	5548.374	−1	5532.292	−4	5517.261	8	5560.717	−6	5544.593	0	5529.501	−1
15.5	5548.414	−9	5531.307	−1	5515.223	−5	5560.783	−2	5543.613	−2	5527.486	2
16.5	5548.414	7	5530.252	−5	5513.148	7	5560.783	−0	5542.572	−2	5525.412	7
17.5	5548.328	−1	5529.138	−4	5510.999	8	5560.717	−2	5541.463	−9	5523.261	−1
18.5	5548.183	−2	5527.964	1	5508.770	−6	5560.593	−0	5540.304	−3	5521.055	−4
19.5	5547.978	−1	5526.721	−1	5506.492	−8	5560.406	2	5539.078	−2	5518.798	4
20.5	5547.708	−1	5525.412	−5	5504.154	−5	5560.157	3	5537.789	−3	5516.463	−4
21.5	5547.377	2	5524.046	−2	5501.763	6	5559.844	3	5536.441	−0	5514.076	−4
22.5	5546.978	−0	5522.616	−1	5499.293	2	5559.471	3	5535.030	−1	5511.635	4
23.5	5546.517	−0	5521.123	−1	5496.761	−2	5559.033	−0	5533.560	0	5509.126	4
24.5	5545.998	4	5519.565	−1	5494.172	1	5558.536	−2	5532.030	2	5506.556	1
25.5	5545.403	−3	5517.944	−2	5491.519	2	5557.988	5	5530.439	2	5503.931	3
26.5	5544.758	2	5516.262	−0	5488.801	−1	5557.371	1	5528.791	3	5501.242	0
27.5	5544.045	3	5514.516	−0	5486.022	−1	5556.705	7	5527.081	1	5498.512	14
28.5	5543.267	1	5512.710	2	5483.182	−1	5555.969	2	5525.319	3	5495.698	−1
29.5	5542.428	1	5510.838	0	5480.278	−2	5555.184	4	5523.498	4	5492.846	4
30.5	5541.535	10	5508.905	1	5477.319	4	5554.338	1	5521.619	2	5489.927	−4
31.5	5540.560	0	5506.908	−0	5474.293	5	5553.436	−4	5519.684	−2	5486.964	−2
32.5	5539.529	−2	5504.851	1	5471.201	2	5552.492	3	5517.700	−2	5483.946	−3
33.5	5538.441	−0	5502.729	−1	5468.048	−2	5551.482	−3	5515.663	−4	5480.880	0
34.5	5537.288	−0	5500.549	−0	5464.839	0	5550.429	−2	5513.576	−4	5477.755	−6
35.5	5536.069	−5	5498.309	3	5461.568	2	5549.326	−1	5511.443	−2	5474.590	−4
36.5	5534.791	−7	5496.000	−0			5548.183	7	5509.264	0	5471.381	−0
37.5	5533.457	−1	5493.634	−0	5454.838	0	5546.978	−1	5507.043	7	5468.134	10
38.5	5532.053	−5	5491.207	0	5451.379	−3	5545.763	25 a	5504.789	23 a	5464.847	23 a
39.5	5530.598	3	5488.719	1	5447.870	3			5502.503	47 a	5461.523	40 a
40.5	5529.068	−4	5486.168	−0					5500.194	88 a		
41.5	5527.486	−0	5483.561	3	5440.642	−13			5497.875	155 a		
42.5	5525.837	−4	5480.880	−7	5436.963	5						
43.5	5524.143	9	5478.156	−1	5433.208	5						
44.5	5522.364	−3	5475.365	−1								
45.5			5472.512	−3								
46.5			5469.607	2								
47.5			5466.637	1								

Note. O-C are observed minus calculated line positions in units of 10^{-3} cm^{-1} and "a" marks perturbed lines.

at 14 920 cm^{-1} in the photoelectron spectrum of VO$^-$ would place the $1^2\Delta$ state at 9370 cm^{-1} above the ground state. The $1^2\Delta$ state would thus lie ∼120 cm^{-1} below the $A^4\Pi$ state. Because the $1^2\Delta$ state has a higher B value than the $A^4\Pi$ state, it would catch up to the $A^4\Pi$ state with increasing rotation, and perturbations similar to those between the $a^2\Sigma^+$ and $B^4\Pi$ states

(*24*) should occur. No avoided crossings have been seen in the $A^4\Pi$ state (*21*), so that any perturbations must occur beyond the observed range of J values. It is also interesting to note that the $1^2\Delta$ state shows anomalous centrifugal distortion, with both spin–orbit components being pushed down at higher J, in the manner expected for interaction with a state just above it.

TABLE 2
Molecular Constants (in cm^{-1}) for the New $^2\Phi$
and $1^2\Delta$ States of VO

State	T_0	B_0	$10^7 \times D_0$	$10^{10} \times H_0$
$^2\Phi_{7/2}$	b+5551.6901(10)	0.520647(16)	6.438(86)	—
$^2\Phi_{5/2}$	a+5539.4643(16)	0.518974(17)	5.997(70)	—
$1^2\Delta_{5/2}$	b	0.552241(17)	6.39(14)	−3.223(53)
$1^2\Delta_{3/2}$	a	0.550894(17)	7.023(94)	−0.133(20)

Note. Numbers in parentheses are one standard deviation in the last digit and "a" and "b" mark undetermined term values of the $1^2\Delta_{3/2}$ and $1^2\Delta_{5/2}$ spin components.

CONCLUSION

The emission spectrum of VO has been observed in the 3400–19 400 cm^{-1} region using a Fourier transform spectrometer. Two new bands observed in the 5400–5600 cm^{-1} interval have been assigned to a new $^2\Phi$–$1^2\Delta$ electronic transition of VO with the 0–0 origins of the $^2\Phi_{5/2}$–$1^2\Delta_{3/2}$ and $^2\Phi_{7/2}$–$1^2\Delta_{5/2}$ subbands located near 5539.46 and 5551.69 cm^{-1}, respectively. The $1^2\Delta$ state is known from the analysis of other near infrared doublet–doublet transitions by Merer *et al.* (*27*). A rotational analysis of the observed subbands provides improved spectroscopic constants for the spin components of the $1^2\Delta$ state. The new $^2\Phi$ excited state has rotational constants of similar magnitude as the $1^2\Phi$ state observed by Merer *et al.* (*27*), and lies in the same energy range. If the new $^2\Phi$ state is the same one as observed in the anion photoelectron spectra of VO$^-$ (*36*), then the $1^2\Delta$ state is located at 9370 cm^{-1} above the ground state. Some *ab initio* calculations on the low-lying doublet states of VO would be most welcome.

ACKNOWLEDGMENTS

REFERENCES

1. M. Grunze, *in* "The Chemical Physics of Solid Surfaces and Heterogeneous Catalysis" (D. A. King and D. P. Woodruff, Eds.), Vol. 4, p. 143. Elsevier, New York, 1982.

2. F. A. Cotton, G. Wilkinson, C. A. Murillo, and M. Bochmann, "Advanced Inorganic Chemistry, A Comprehensive Text," 6th ed., Wiley, New York, 1999.

3. C. Jascheck and M. Jascheck, "The Behavior of Chemical Elements in Stars." Cambridge Univ. Press, Cambridge, UK, 1995.

4. A. J. Merer, *Annu. Rev. Phys. Chem.* **40,** 407–438 (1989).

5. P. W. Merrill, A. J. Deutsch, and P. C. Keenan, *Astrophys. J.* **136,** 21–34 (1962).

6. H. Machara and Y. Y. Yamashito, *Pub. Astron. Soc. Jpn.* **28,** 135–140 (1976).

7. D. L. Lambert and R. E. S. Clegg, *Mon. Not. R. Astron. Soc.* **191,** 367–389 (1978).

8. S. Wyckoff and R. E. S. Clegg, *Mon. Not. R. Astron. Soc.* **184,** 127–143 (1978).

9. N. M. White and R. F. Wing, *Astrophys. J.* **222,** 209–219 (1978).

10. A. J. Sauval, *Astron. Astrophys.* **62,** 295–298 (1978).

11. J. M. Brett, *Astron. Astrophys.* **231,** 440–452 (1990).

12. R. M. Wenzcovitch, W. W. Schultz, and P. B. Allen, *Phys. Rev. Lett.* **72,** 3389–3392 (1994).

13. J. C. Parker, U. W. Geiser, D. J. Lam, Y. N. Xu, and Y. C. Wai, *J. Am. Ceram. Soc.* **73,** 3206 (1990).

14. P. I. Sorantin and K. Schwartz, *Inorg. Chem.* **31,** 567–576 (1992).

15. M. F. Becker, B. A. Buckman, R. M. Walser, T. Leping, P. Georges, and A. Brun, *Appl. Phys. Lett.* **65,** 1507–1509 (1994).

16. J. LeBars, J. C. Vedrine, A. Auroux, B. Pommier, and G. M. Pajonk, *J. Phys. Chem.* **96,** 2217–2221 (1992).

17. G. V. Chertihin, W. D. Bare, and L. Andrews, *J. Phys. Chem.* **101,** 5090–5096 (1997).

18. J. Xu, M. T. Rodgers, J. B. Griffin, and P. B. Armentrout, *J. Chem. Phys.* **108,** 9339–9350 (1998).

19. K. D. Carlson and C. Moser, *J. Chem. Phys.* **44,** 3259–3265 (1966).

20. C. W. Bauschlicher and S. R. Langhoff, *J. Chem. Phys.* **85,** 5936–5942 (1986).

21. A. S.-C. Cheung, A. W. Taylor, and A. J. Merer, *J. Mol. Spectrosc.* **92,** 391–409 (1982).

22. G. Huang, A. J. Merer, and D. J. Clouthier, *J. Mol. Spectrosc.* **153,** 32–40 (1992).

23. A. S.-C. Cheung, P. G. Hajigeorgiou, G. Huang, S.-Z. Huang, and A. J. Merer, *J. Mol. Spectrosc.* **163,** 443–458 (1994).

24. A. G. Adam, M. Barnes, B. Berno, R. D. Bower, and A. J. Merer, *J. Mol. Spectrosc.* **170,** 94–130 (1995).

25. A. S.-C. Cheung, R. C. Hansen, A. M. Lyyra, and A. J. Merer, *J. Mol. Spectrosc.* **86,** 526–533 (1981).

26. A. S.-C. Cheung and A. J. Merer, *Mol. Phys.* **46,** 111–128 (1982).

27. A. J. Merer, G. Huang, A. S.-C. Cheung, and A. W. Taylor, *J. Mol. Spectrosc.* **125,** 465–503 (1987).

28. R. D. Suenram, G. T. Fraser, and F. J. Lovas, *J. Mol. Spectrosc.* **148,** 114–122 (1991).

29. L. Karlsson, B. Lindgren, C. Lundevall, and U. Sassenberg, *J. Mol. Spectrosc.* **181,** 274–278 (1997).

30. J. M. Dyke, B. W. Gravenor, M. P. Hastings, and A. Morris, *J. Phys. Chem.* **80,** 4613–4617 (1985).

31. G. Balducci, G. Gigli, and M. Guido, *J. Chem. Phys.* **79,** 5623–5627 (1983).

32. M. Farber, O. M. Uy, and R. D. Srivastava, *J. Chem. Phys.* **56,** 5312–5315 (1972).

33. J. Harrington and J. C. Weisshaar, *J. Chem. Phys.* **97,** 2809–2812 (1992).

34. L. B. Knight, R. Babb, M. Ray, J. T. Banisaukas, L. Russon, R. S. Dailey, and E. R. Davidson, *J. Chem. Phys.* **105,** 10 237–10 250 (1996).

35. J. D. Weinstein, R. DeCarvalho, K. Amar, A. Boca, B. C. Odom, B. Friedrich, and J. M. Doyle, *J. Chem. Phys.* **109,** 2656–2661 (1998).

36. H. Wu and L. S. Wang, *J. Chem. Phys.* **108,** 5310–5318 (1998).

37. A. G. Maki and J. S. Wells, "Wavenumber Calibration Tables from Heterodyne Frequency Measurements," NIST Special Publication 821. U.S. Government Printing Office, Washington, DC, Dec. 1999.

38. R. S. Ram, P. F. Bernath, and S. P. Davis, *J. Chem. Phys.* **114,** 4457–4460 (2001).

39. R. S. Ram, P. F. Bernath, and S. P. Davis, *J. Mol. Spectrosc.* **210,** 110–118 (2001).